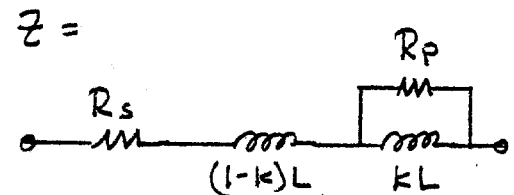
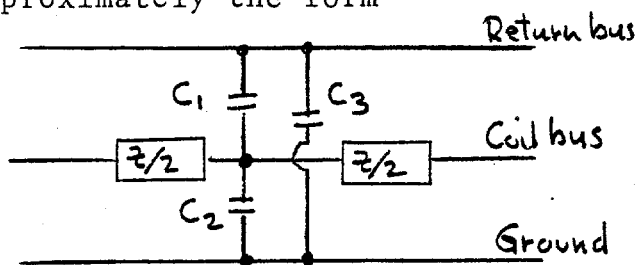


UPC 037

TRANSMISSION LINE CHARACTERISTICS OF
ENERGY DOUBLER DIPOLE STRINGS

Upon realization that the relatively high inductance per dipole (≈ 50 mH) and capacitance to ground (≈ 60 nF) can lead to relatively low frequency (~ 12 Hz) high Q standing waves in a 774 dipole string, this study was undertaken to understand what oscillation modes would dominate, how power supply location and ramping would excite them, and how appropriately placed damping resistors could control them.

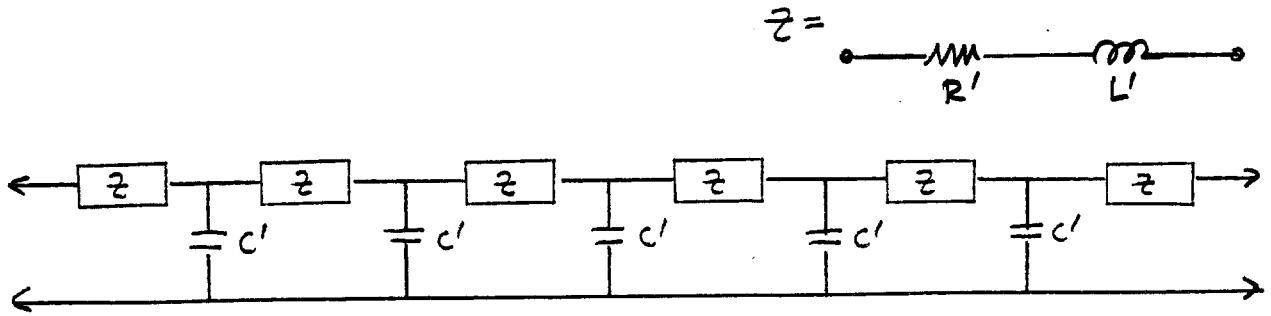
Studies of the electrical characteristics of individual superconducting ED dipoles indicate that their equivalent circuit is approximately the form ¹



Approximate values are:

$L = 45$ mH	$C_1 = 6$ nF	
$k = 0.65$	$C_2 = 58$ nF	(1)
$R_p = 50$ Ω	$C_3 = 0.7$ nF	
$R_s = 0$ Ω		

In reality, the ED dipole is a 6 terminal device, but as the inductance and eddy current losses of the coil bus so dominate the series impedance characteristics of the 3 conductors, it is probably safe to consider both the return bus and ground as having neither resistance nor inductance. Once that assumption is made, then it is apparent that neither conductor can have a potential gradient, leading to a much simplified transmission line model:



where $Z = R' + j\omega L'$;
 $R' = R_s + \frac{kL\tau\omega^2}{1+\omega^2\tau^2}$; $L' = (1-k)L + \frac{kL}{1+\omega^2\tau^2}$
 (both R' and L' are functions of ω) (2)
 $Y = j\omega(C_1+C_2) = j\omega C'$
 $\tau = kL/R_p$

Using $e(x,t)$ and $i(x,t)$ as the time and position dependent voltage and current, we have the following differential equations

$$\frac{\partial e(x,t)}{\partial x} = -R' i(x,t) - L' \frac{\partial i(x,t)}{\partial t}$$

and

$$\frac{\partial i(x,t)}{\partial x} = -C' \frac{\partial e(x,t)}{\partial t}$$

(3)

By differentiating the above equations by x and t and making appropriate substitutions we have

$$\frac{\partial^2 e(x,t)}{\partial x^2} = L'C' \frac{\partial^2 e(x,t)}{\partial t^2} + R'C' \frac{\partial e(x,t)}{\partial t}$$

and

$$\frac{\partial^2 i(x,t)}{\partial x^2} = L'C' \frac{\partial^2 i(x,t)}{\partial t^2} + R'C' \frac{\partial i(x,t)}{\partial t}$$

(4)

Consider solutions of the form

$$e(x,t) = E(x) e^{j\omega t} \quad i(x,t) = I(x) e^{j\omega t}$$

Substitutions in the above equations yield

$$\frac{d^2 E(x)}{dx^2} - \gamma^2 E(x) = 0$$

$$\frac{d^2 I(x)}{dx^2} - \gamma^2 I(x) = 0$$

[5]

where $\gamma^2 = j\omega C'(R' + j\omega L') = Y \cdot Z$

The general solutions to the above equations are:

$$\begin{aligned} E(x) &= A_1 e^{-\gamma x} + A_2 e^{\gamma x} \\ I(x) &= B_1 e^{-\gamma x} + B_2 e^{\gamma x} \end{aligned} \quad [6]$$

Substituting the complete solutions $e(x,t)$ and $i(x,t)$ into equation

(3) yields $-\gamma A_1 + \gamma B_1 = 0 \Rightarrow B_1 = A_1 / z_0$ [7]

and $\gamma A_2 + \gamma B_2 = 0 \Rightarrow B_2 = -A_2 / z_0$

and

where $z_0 = Z / \gamma = \sqrt{Z / Y}$

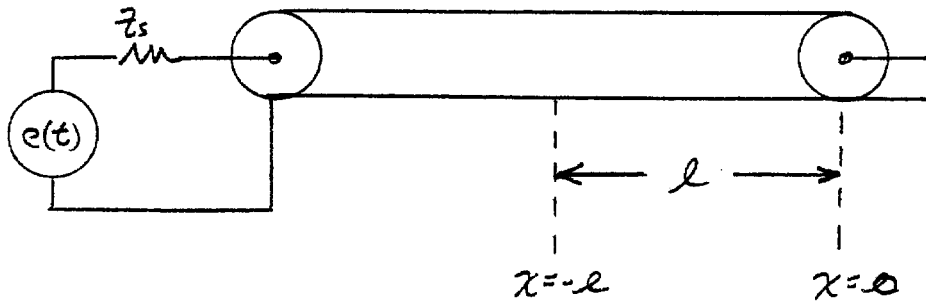
Hence the complete solutions for a transmission line are:

$$\begin{aligned} e(x,t) &= [A_1 e^{-\gamma x} + A_2 e^{\gamma x}] e^{j\omega t} \\ i(x,t) &= \left[\frac{A_1}{z_0} e^{-\gamma x} - \frac{A_2}{z_0} e^{\gamma x} \right] e^{j\omega t} \end{aligned} \quad [8]$$

where $z_0 = \sqrt{Z / Y}$ and $\gamma = \sqrt{Z \cdot Y}$

(both z_0 and γ are complex and dependent on ω)

We now consider a long transmission line shorted at one end:



$e(0,t) = 0$ leading to the boundary condition $A_2 = -A_1$

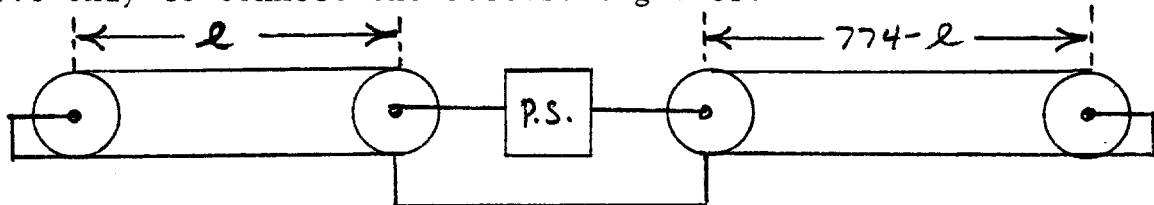
Hence we can write down the transmission line impedance at a distance l from the end:

$$Z(l, \omega) = \frac{e(l,t)}{i(l,t)} = z_0 \frac{e^{\gamma l} - e^{-\gamma l}}{e^{\gamma l} + e^{-\gamma l}} = z_0 \tanh(\gamma l) \quad [9]$$

It should be pointed out at this time that l is in "natural" units; 1 natural unit is 1 dipole, as the units of γ are (dipoles)⁻¹.

We now consider one of several voltage regulated power supplies in a

series connected string of 774 dipoles. We calculate the impedance as seen by one supply located a distance l from one end of the string with both ends shorted. The other supplies in the string are assumed to have a very low impedance compared to the dipoles, and therefore serve only to connect the sectors together.



Due to the series connection of the power supply, it sees the sums of the input impedances of the two transmission lines, hence

$$Z(774, l, \omega) = Z_0 [\tanh(\gamma l) + \tanh \gamma (774 - l)] \quad [10]$$

Even though both Z_0 and γ are complex and frequency dependent, this closed-form expression is easily evaluated as complex notation and circular functions of complex numbers are easily manipulated in FORTRAN.

We are now in a position to examine the l, ω plane for frequencies and power supply locations which can couple to resonances. We neglect the effect of quadrupoles on the coil bus as their inductance is about 15% of the dipole inductance and they are roughly only 1/4 as numerous, hence probably changing the characteristic impedance and resonant frequencies by about 2%.

We can now estimate some characteristics of the 774 dipole string. Its low frequency (i.e., $\omega\tau \ll 1$ in equation (2)) characteristic impedance is:

$$Z_0 = \sqrt{Z/Y} = \sqrt{L'/C'} = \sqrt{\frac{.045}{6.4 \times 10^{-8}}} = 840 \text{ ohms.}$$

and the corresponding velocity of propagation is

$$v = \sqrt{\frac{-\omega^2}{Y \cdot Z}} = \sqrt{1/L'C'} = 1.86 \times 10^4 \text{ dipoles/sec}$$

The lowest order mode of oscillation is expected to be a $\lambda/2$ standing wave with voltage nodes at the ends. The frequency at which this would occur is:

$$f = \frac{nv}{2l} = \frac{1.86 \times 10^4}{2 \times 774} = 12 \text{ Hz.} \quad n = 1/2 \text{ mode}$$

As L' is frequency dependent (it decreases with increasing frequency), we should expect Z_0 to decrease with increasing ω , and v to increase. In addition, as R' increases with frequency, the real part of γ increases, leading to increased attenuation.

It is quite instructive to examine the positional as well as the frequency dependence of equation (10). Using the values for all the elements in the dipole (equation (1)), we can calculate the impedance seen by the power supply as a function of ω and l . This is shown in figure 1. The notation used in the figure emphasizes the low impedance points, i.e., the points where the impedance is significantly below $2Z_0$, the impedance the power supply would see if the two dipole strings were infinitely long. These points represent current maxima (voltage nodes) of standing waves, and indicate points where a significant amount of power can be transferred to the transmission line from the power supply. The Q of the $\lambda/2$ standing wave is over 30, and decreases for higher order standing waves ($\frac{n\lambda}{2}$). This is due to the ω^2 dependence of R' in equation (2). The specific reasons for the high Q and low resonant frequencies relative to the Main Ring are that the ED dipole inductance is an order of magnitude higher than the main ring dipoles, and that the ED dipoles have virtually no coil resistance.

Although frequency domain analysis is suitable for establishing the characteristics of resonances, and understanding the effects of power supply ripple on magnetic field quality, it is not adequate for understanding how the standing wave modes are excited and damped under

ramping (i.e., constant dI/dt) conditions. To carry out the necessary Laplace transforms, we use a computer program SPICE, developed at Berkeley to calculate DC, AC, and transient analysis of complex electrical and electronic circuits. In SPICE, the circuit to be analyzed is specified, which in our case ideally consists of 774 dipoles of roughly 7 components each, and the time dependence of one or more power supplies in the circuit is specified. The time dependence may be either a voltage step (current ramp) or a voltage ramp (current parabola).

In reality, 5400 components makes excessive demands on computer CPU time and core, so a reasonable approximation is to model a magnet string of 96 cells, each cell representing 8 dipole magnets. Tests on this cell model indicate that there is very little difference from the original model where each magnet is represented individually.

In the cell model, the distinctness of the return bus and ground is maintained for two reasons (see illustration on page 1): Power supply arrangements which are not symmetric relative to the ends of the dipole string create a DC voltage potential on the return bus relative to ground during ramping; and at the ends the coil bus is shorted to the return bus only, with the connection between the return bus and ground open (actually it is a free parameter in the circuit analysis). As will be seen, this has important consequences with regard to the amplitude of the $\lambda/2$ resonance.

In reality, the capacitance to "ground" is actually capacitance to the stainless steel cellars and the stainless steel bore tube, both at liquid He temperatures. The continuity of this ground from one magnet to the next is via vacuum couplings which are assumed to be adequate to handle the currents normally encountered during ramping (less than 1 amp). This current is the result of a current difference between

the coil bus current and the return bus current during transients. In addition, the connection between these cryogenic parts and the external ground is via low heat loss stainless steel tubes at the end of every magnet (in the coupler box). Again, this connection is more than adequate to carry the normal currents encountered during ramping, but is (demonstrated) not adequate to carry high currents in the event of a magnet failure leading to high ground currents. Failure mode analysis is outside the scope of this note.

The actual transient analysis was carried out in two parts. In part 1, the 96 cells were divided into 4 groups of 24 cells each, and a power supply was placed at the end, then at the center, then at the 25% point to observe what influence power supply location had on the excitation of the various modes of oscillation. A damping resistor was then installed across the coil and its effect was analyzed. In part 2, the 96 cells were divided up into an arrangement such that the transmission line was terminated at cell #A0 and #F34, with power supplies located at service buildings A1, B1, C1, D1, E1, and F1. Both voltage steps and voltage ramps were tested, with and without damping resistors. Figure 2 presents the actual model used for the part 1 analysis. The supply had a small series reactive filter shunted by 10 ohms to provide some ripple filtering. The effect of this filter on the excitation of the dominant standing wave modes is negligible. The cell model as shown represents 8 dipoles with the distinct nature of the return bus and ground preserved. Most resistors (RA-RO, RTR1, and RTR2) are 10^{-6} ohms, placed in the circuit in order to monitor current. A separate reference line was needed due to idiosyncracies of the program, but does not affect the analysis. The supply shown at one end, was moved to other locations during the transient analysis. In addition the termination of the coil bus to ground at each end was

varied from a few ohms to ∞ , and the damping resistor was varied from roughly 100 ohms to ∞ . Although presentation of all the transient plots would be helpful, only a few are actually shown as being representative.

In Figure 3A a power supply is located at one end of the string, and a 1000 volt step is applied at $t=0$. The coil bus to ground is unterminated at both ends ($RTG1 = RTG2 = \infty$) and no damping resistor is used. The 5 curves show the currents at the 5 points along the transmission line (0,24,48,72, and 96 cell points). For this case $dI/dt = \frac{1000}{96 \times .36} = 29$ Amps/sec. It is seen that the peak-to-peak standing wave oscillation is about 0.6 amps, with current minima at or near the 25% and 75% points. The currents are maximum at the ends and at the center with the latter being 180° out of phase, a $\frac{n\lambda}{2} = \lambda$ mode. The period is about 43 msec ($f = 23$ Hz). In Figure 3B the voltages at the same 5 points are presented showing a maximum amplitude of about 500 volts peak-peak at the current nodes. Very little sign of the 12 Hz $\frac{\lambda}{2}$ mode is seen. If however, the return bus is shorted to ground at the 50% point, the $\frac{\lambda}{2}$ mode dominates, indicating that information is traveling along the transmission line mode return bus/ground, and cancelling this mode. It seems to be important that the distinctness of these two lines be maintained. The approximate transmission line impedance can be seen by the relative voltage and current amplitudes of the standing wave: $Z_0 \sim 500$ volts/-6 amps ~ 800 ohms. The peak current seen traveling along the ground circuit (representing an equivalent current difference between the coil bus and the return bus) is about 0.5 Amps. Terminating the coil/ground transmission mode with its characteristic impedances removes the last vestiges of the $\frac{\lambda}{2}$ mode, it has a very undesirable feature in that an asymmetrically

located supply can then induce excessive voltages to ground. In figure 3B, the maximum voltage to ground is ± 500 volts; when the terminations are installed it becomes $+1000-0$. The relatively high Q of this standing wave resonance is apparent in that the oscillation is poorly damped.

Figures 4A and 4B are similar to Figures 3A and 3B except that a 160 ohm/cell (20 ohms/dipole) damping resistor is installed. Voltages are seen to have nearly reached their steady-state (ramping) voltages within 100 msec, and the standing currents are estimated to be less than 100 ma (p-p). Results with the supply placed at the 25% point are qualitatively similar except that the positions of the current and voltage nodes in the 23 Hz oscillation are shifted in position.

In part II of the analysis, we use the circuit shown in Figure 5. Each of 6 power supplies is stepped or ramped to 1670 volts (giving a total of 10 kV around the ring, and a dI/dt of 290 Amps/sec). The power supplies are asymmetrically located in order to be compatible with a convenient assignment of Service Buildings and location of the ends of the transmission line.

In the first case tried (no damping resistor, open termination at ends) the maximum voltage oscillation seen was about 100 volts p-p, implying roughly 100 ma of standing wave at 23 Hz (this current is too small to be seen directly at 290 Amps/sec ramp rate). When the damping resistor was installed (again 160 ohms/cell), the results shown in figure 6A, B, and C were obtained. Figure 6A shows the current at 4 selected positions along the string. Figure 6B shows the voltages at both the + and - terminals of 3 supplies (note that the return bus is at about -500 volts, leading to roughly 1300 volts potential difference in certain magnets). If the power supply voltages were increased to provide a 400 Amp/sec ramp, these voltages would be

increased accordingly. Figure 6c shows the voltages on the positive terminals of all six power supplies (note expanded scale) indicating that the oscillation is roughly 10 volts (p-p) after 100 millisecc. Much of the decrease in amplitude relative to the earlier model with one supply is due to destructive interference of the oscillations generated by each individual supply. This amplitude implies a current oscillation of about 15 ma.

Figures 7A, B, and C are similar to 6A, B, and C except that the power supplies are ramped from 0 volts to 1670 volts (10 kV total round ring) over a 100 msec period. Current oscillations at any point are not discernable but analysis of figure 7C implies 10 ma. maximum current about 10 millisecc. after beginning of power supply ramping.

CONSEQUENCES OF DAMPING RESISTOR

A damping resistor of the order of 20 ohms shunting the dipole coil (actually an 80 ohm resistor shunting a half cell) will cause a current retardation in the coil of about $\tau = \frac{L}{R} = \frac{.045}{20} = 2.25$ millisecc. With a ramp rate of 400 Amps/sec, the current in the damping resistor would be

$$I_R = \tau(dI/dt) = 0.9 \text{ Amps.}$$

As these resistors would include the quadrupole in every half cell as well as the 4 dipoles, there is no obvious net effect on the tune of the machine. However, if any resistor is removed for any reason, the currents in that half cell would be increased by 0.9 Amps. The total power would be

$I^2R = .9^2 \times 80 = 65$ watts per resistor, or roughly 6.5 kw for the entire ring. This resistor would be outside the magnet, probably coupled between the quench buses at each half cell and therefore would not contribute to the heat load on the cryogenic

system. This loop would of course include the return yoke of the dipoles (1 amp turn). This is not thought to be serious either in terms of the expected inductance (≈ 1 mHy) or in terms of unbalancing the flux in the yoke.

CONCLUSION

There does not appear to be any serious problem regarding a 774 dipole string of superconducting magnets. Power supply location relative to the ends is important in order to minimize the voltages occurring between the coil and return bus during ramping, and maintaining the distinctness of the return bus and ground is important to minimize the 12 Hz $\lambda/2$ mode. A damping resistor of the order of 20 ohms per dipole seems adequate.

This note has specifically avoided discussing the effects of power supply ripple, which will be reviewed elsewhere. Ripple may place more restrictive demands on the damping resistor for example. Also avoided is the subject of fault analysis, i.e., what kind of faults could occur, and what kind of transients might be induced.

1. "Study of eddy current effects in Energy Doubler Dipole Magnets"
(R. Shafer) Design Report # UPC-31

RES/nep

FIGURE 1 Magnitude of $Z(\omega, \ell)$ vs. ω and ℓ

- *** $Z(\omega, \ell) \leq 200$ ohms
- ** $200 < Z(\omega, \ell) \leq 500$ ohms
- * $500 < Z(\omega, \ell) \leq 1000$ ohms

Frequency F (Hz)

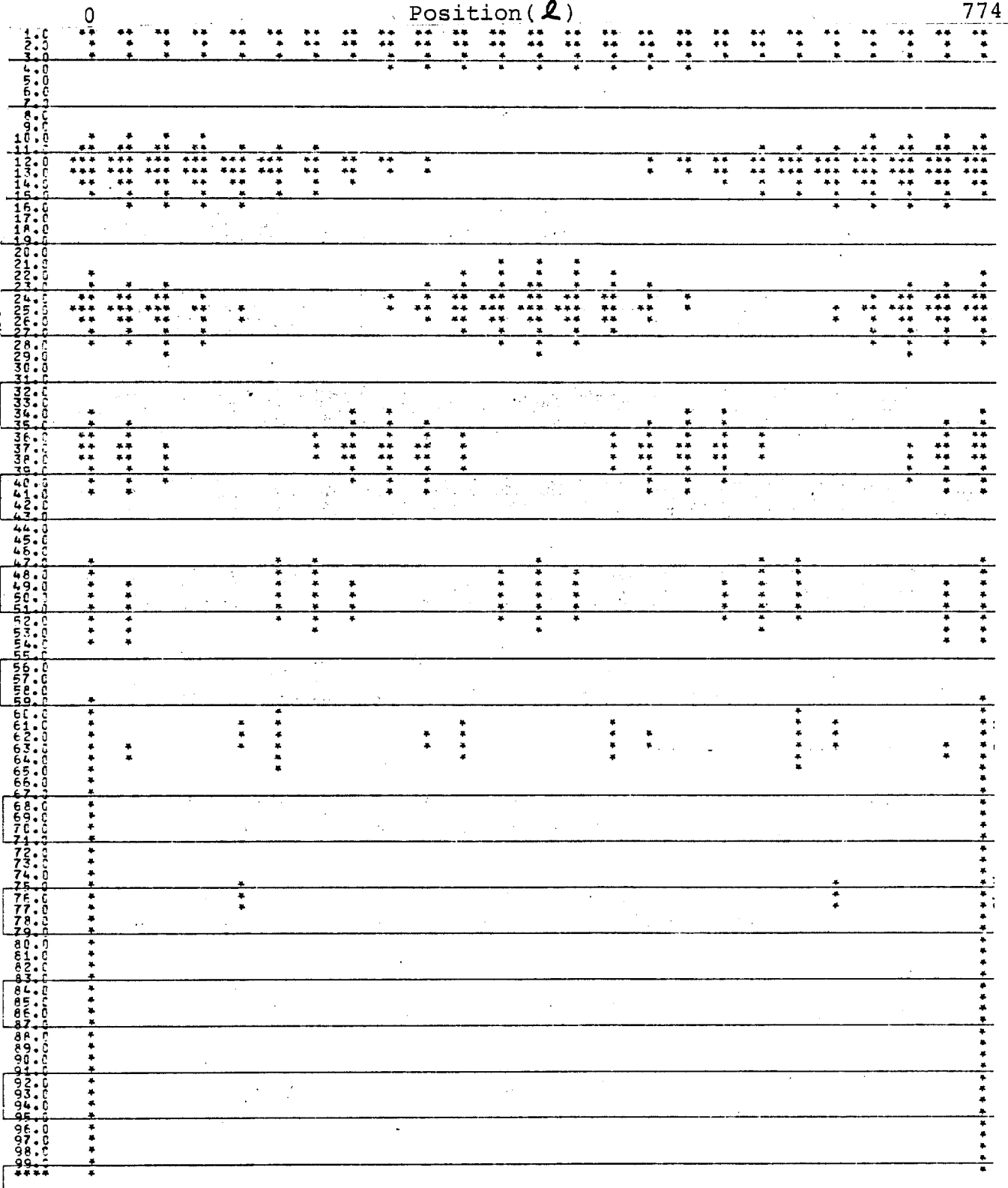
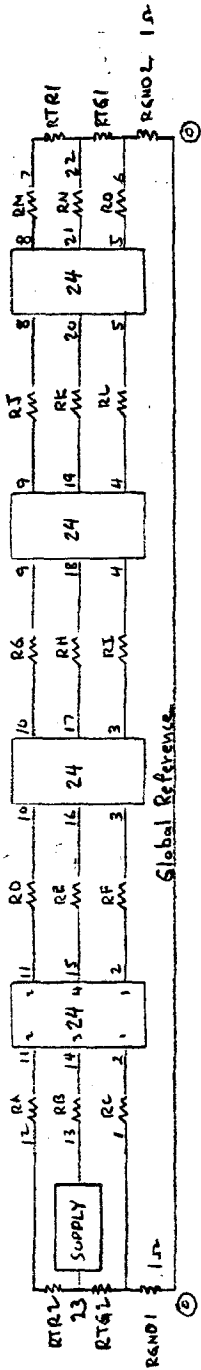
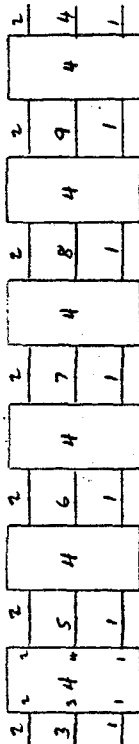


FIGURE 2: Block diagram of circuit used in part I of transient analysis

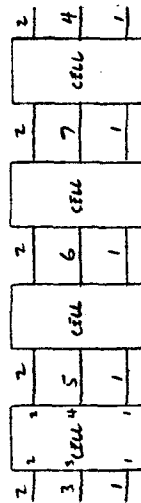
	NATIONAL ACCELERATOR LABORATORY	SECTION	PROJECT	SERIAL-CATEGORY	PAGE
	ENGINEERING NOTE				
SUBJECT		NAME <i>Shafiq</i>			
Doubler Ring Version I (Model for transient Anal.)		DATE	REVISION DATE		
		12/1/78			



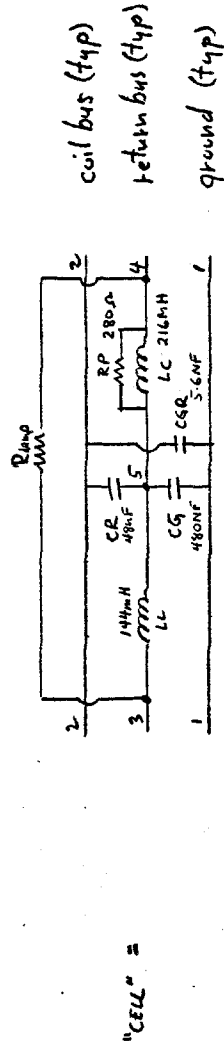
All resistors
 RA-RO are $1 \mu\text{ohm}$
 RTG1, RTG2 = 100Ω to ∞
 $R_{\text{damp}} = 80 \Omega$ to ∞



"Two Four" =



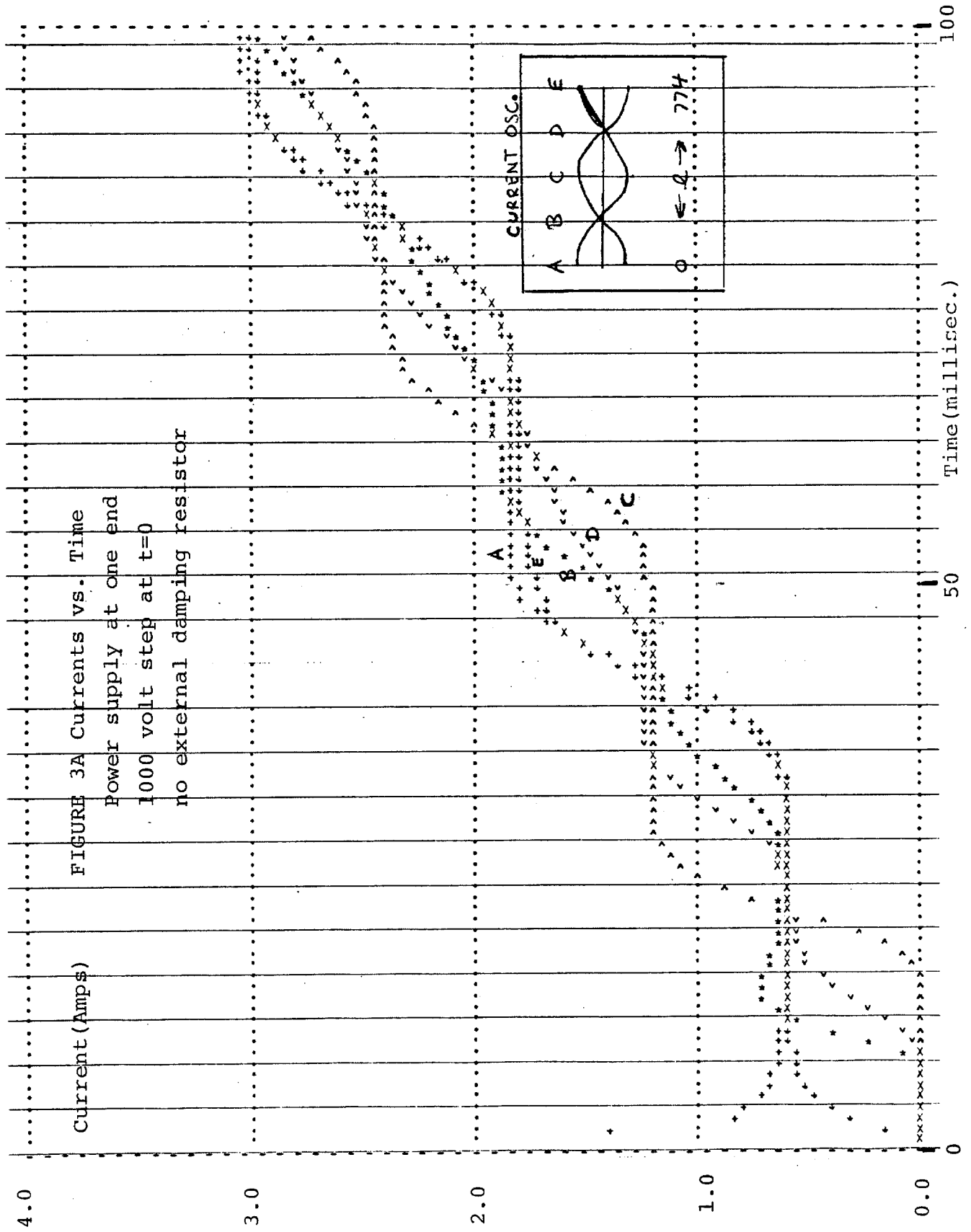
"Four" =

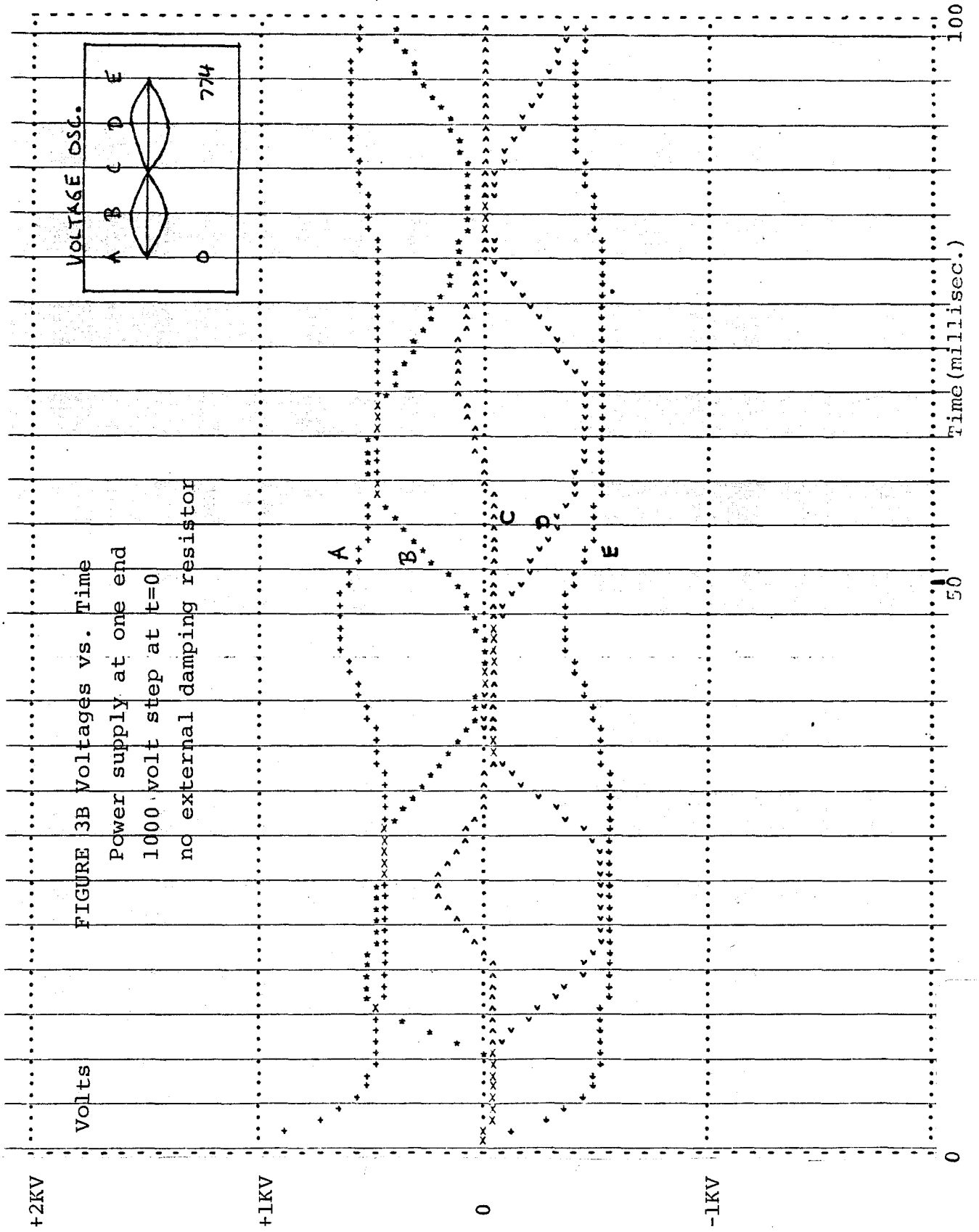


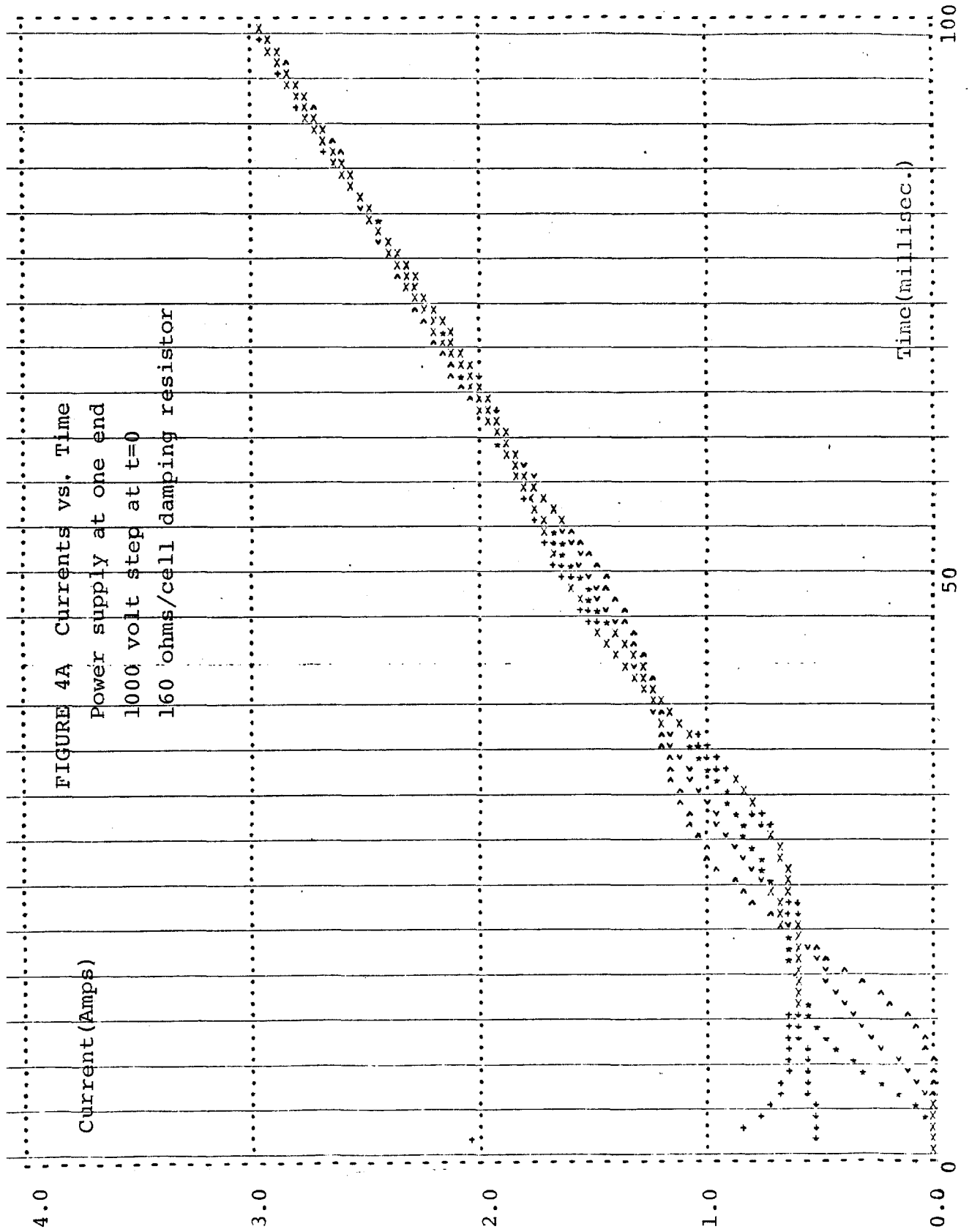
"CELL" =

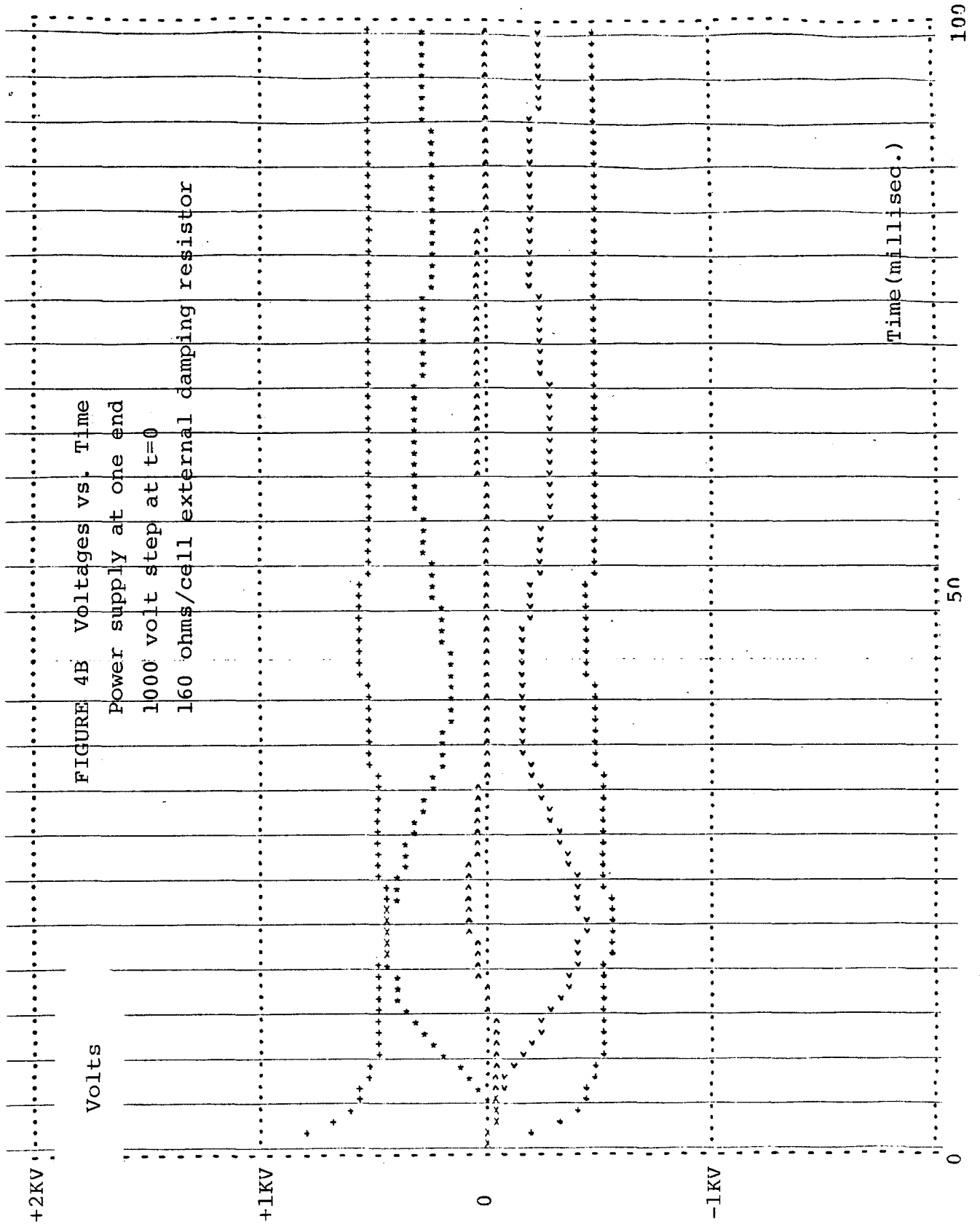


"Supply" =



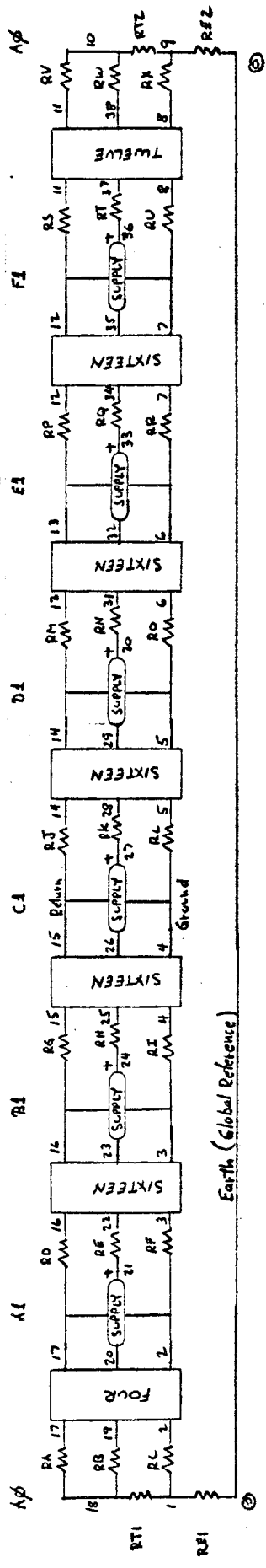




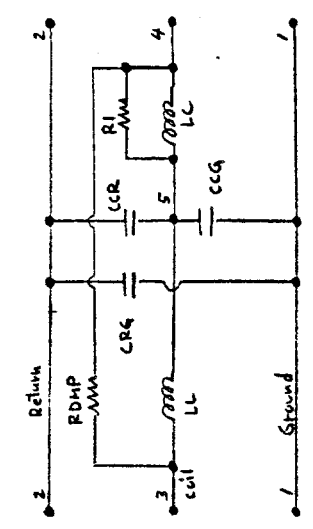
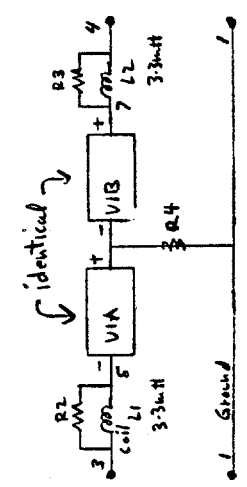
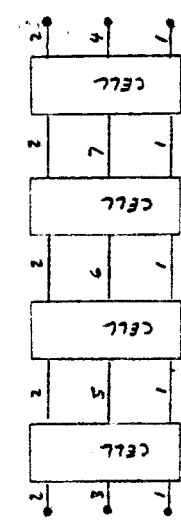
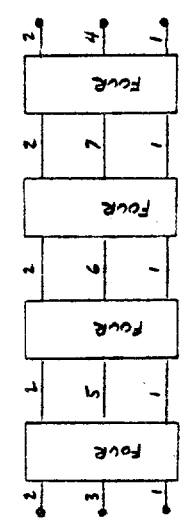
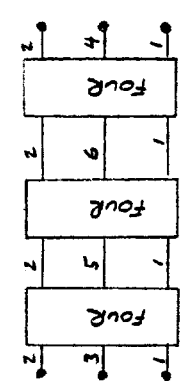


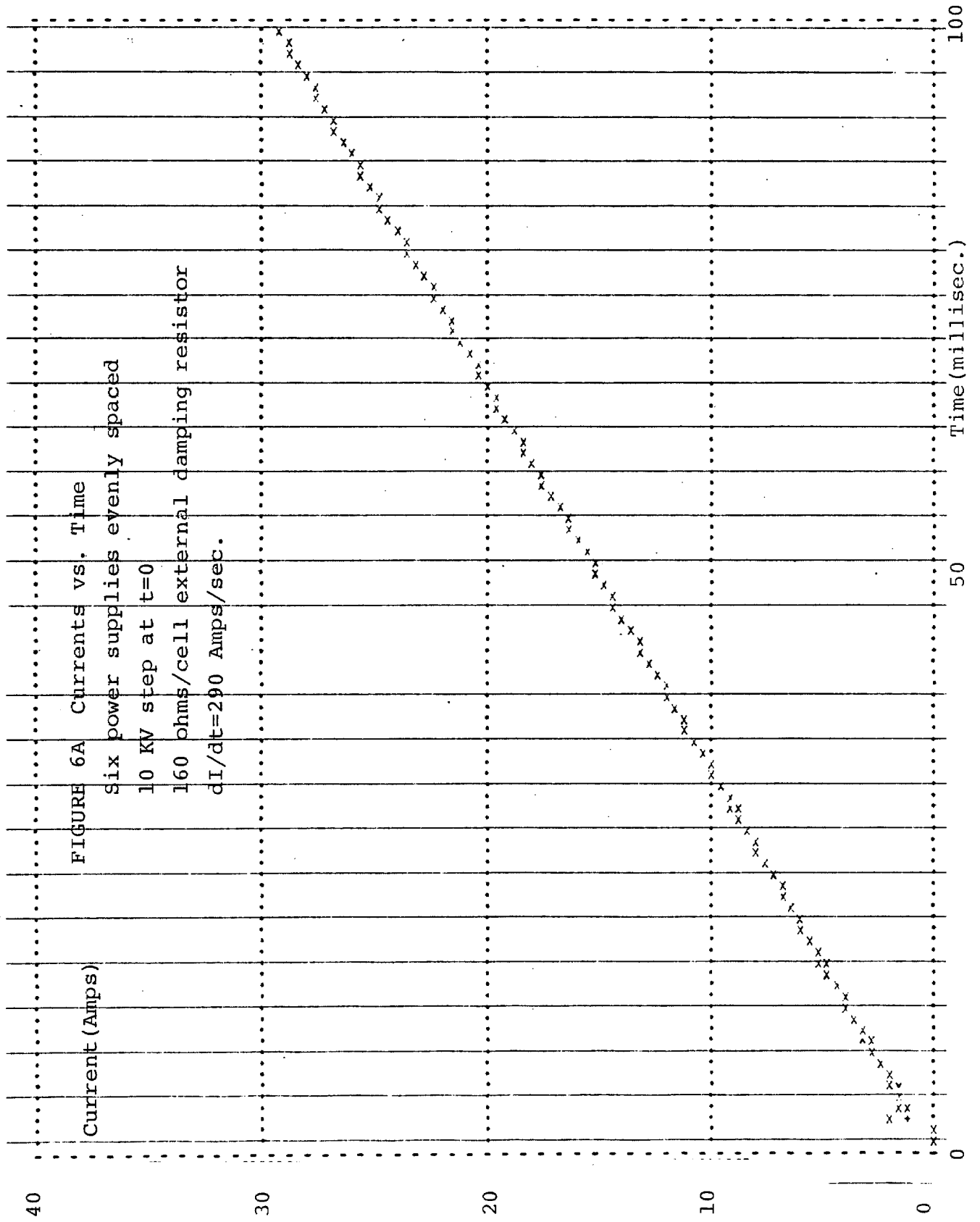
	NATIONAL ACCELERATOR LABORATORY	SECTION	PROJECT	SERIAL-CATEGORY	PAGE
	ENGINEERING NOTE				
SUBJECT	Doubler Ring Version II (model for transient analysis)				
	NAME	Shahar	DATE	12/4/78	REVISION DATE

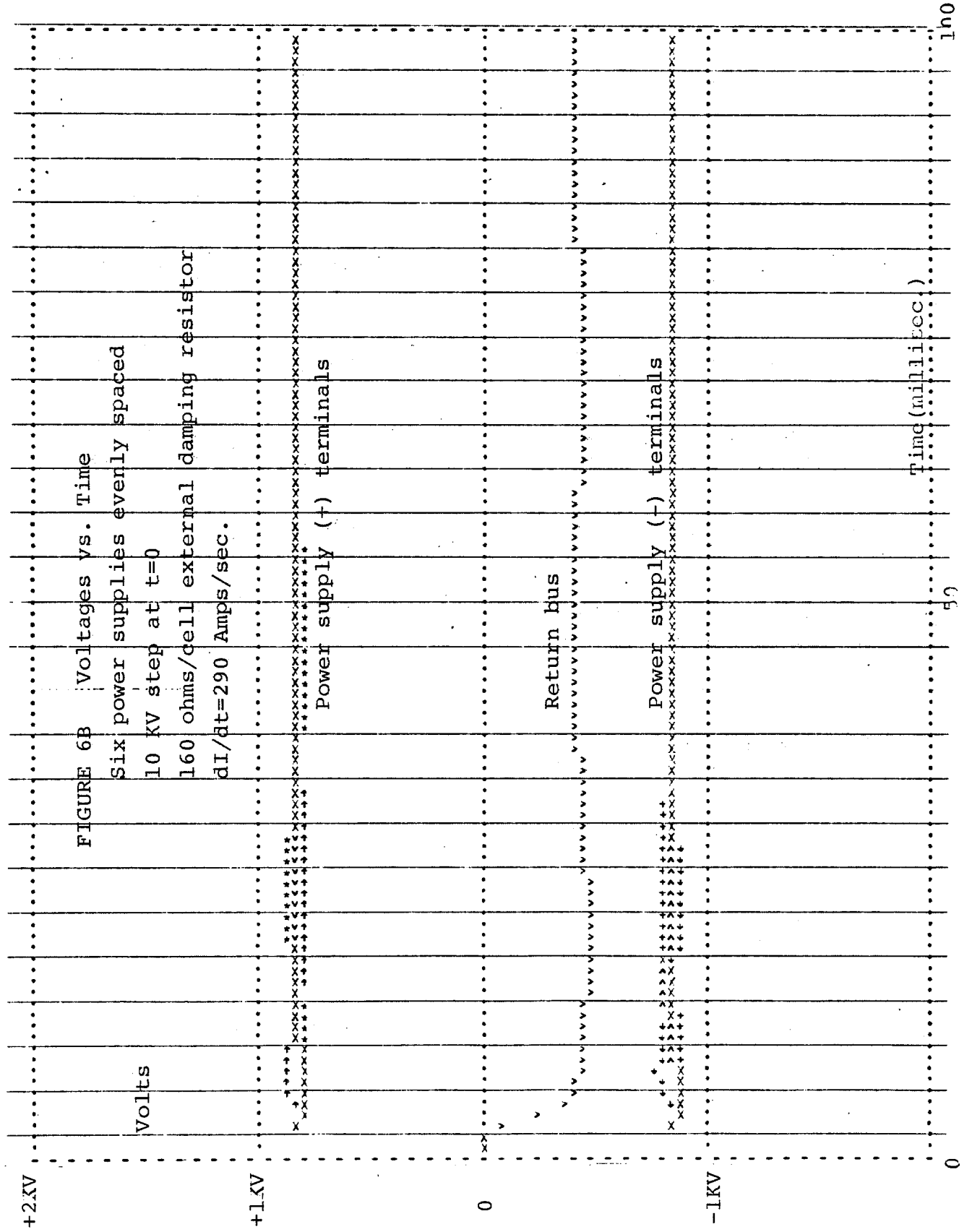
FIGURE 5: Block diagram of circuit used in part II of transient analysis.

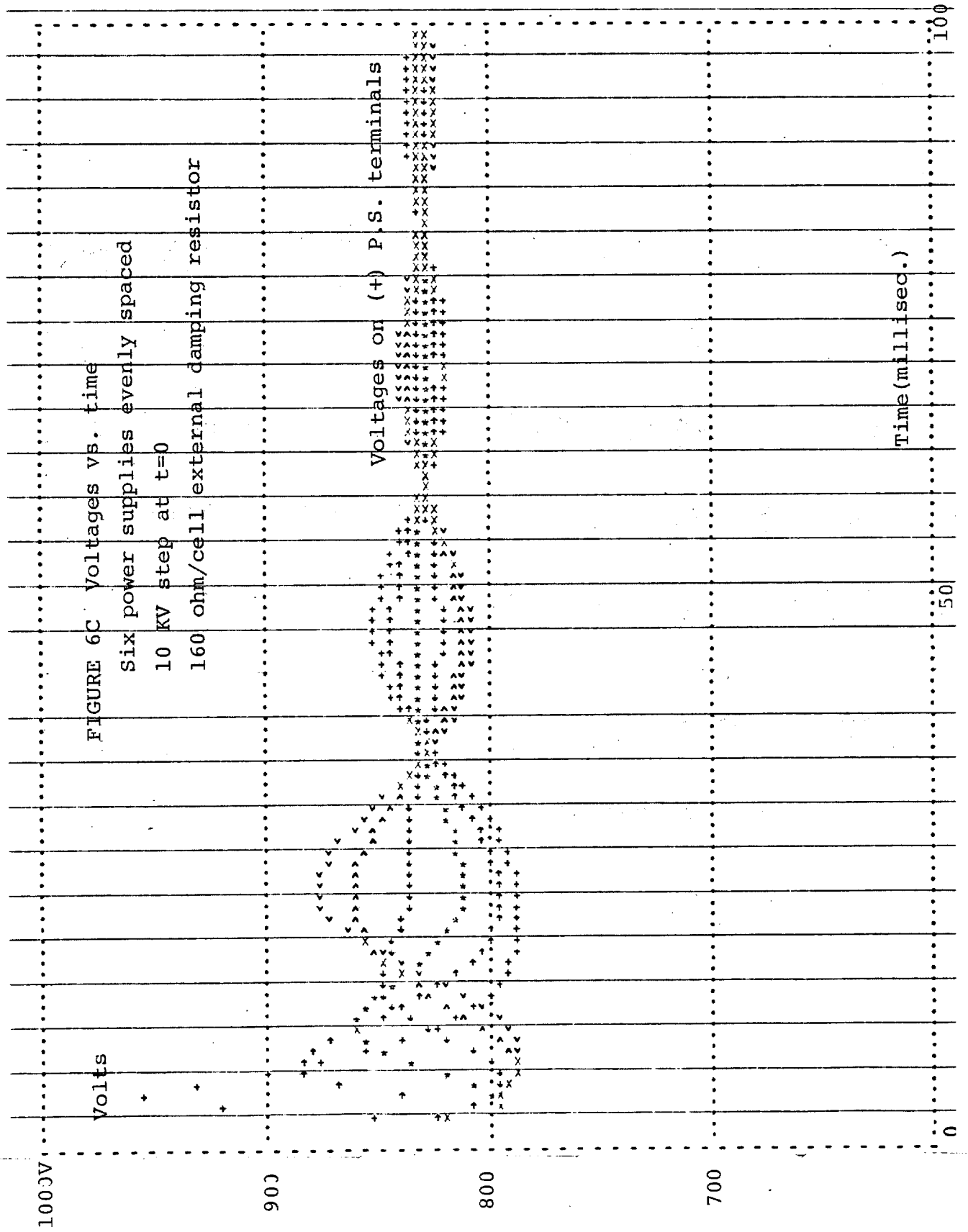


- RA-RX 100HM
- RT,RT2 open
- RE,REL 1 ohm
- RI 35 ohm x 8
- RT,RT3 10 ohm
- R4 10k ohm
- LL .4x45MH x 8
- LC .6x45MH x 8
- RDMP 20Ω x 8 → ∞
- CR4 .7MF x 8
- CC4 60NF x 8
- CCR 6MF x 8









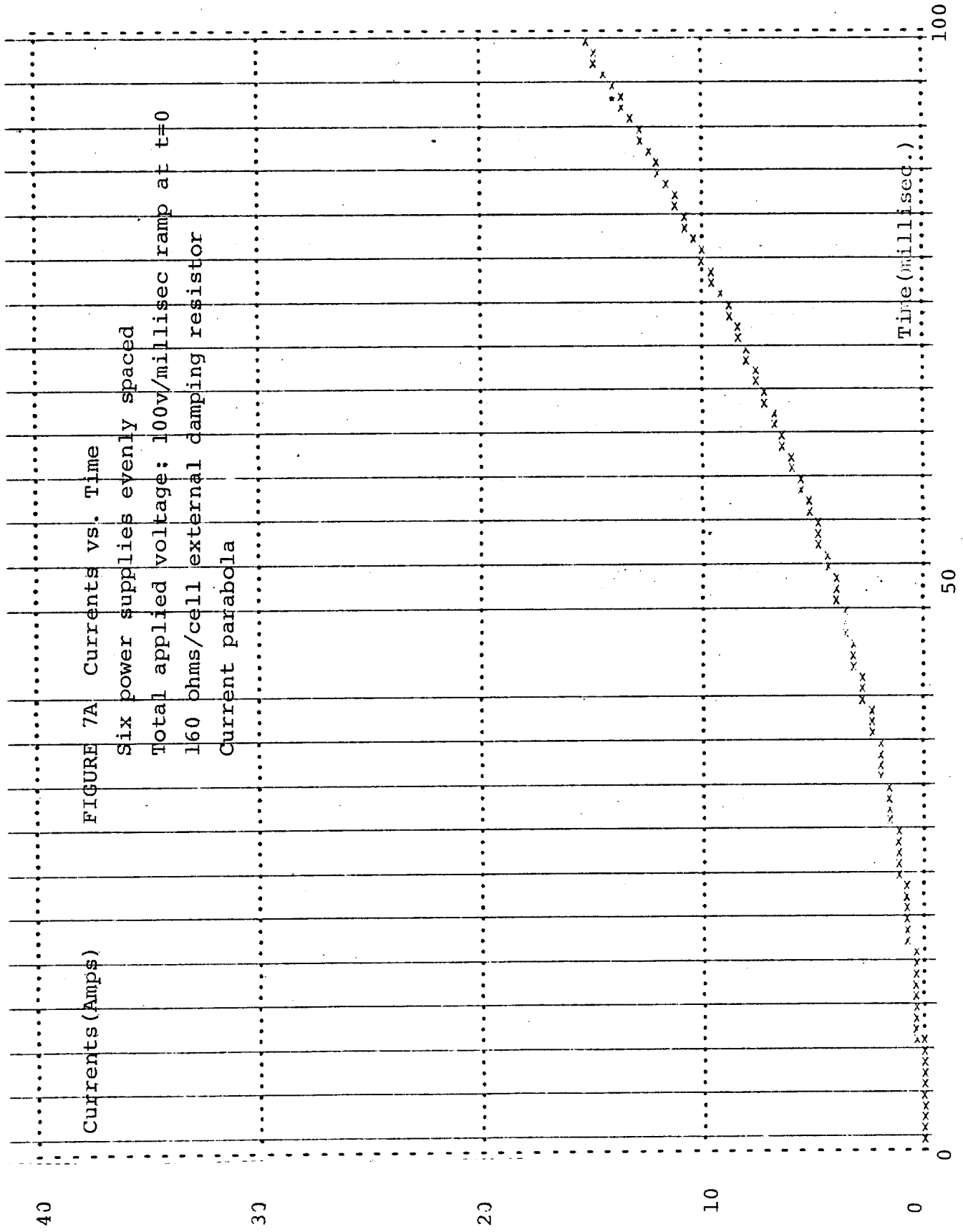
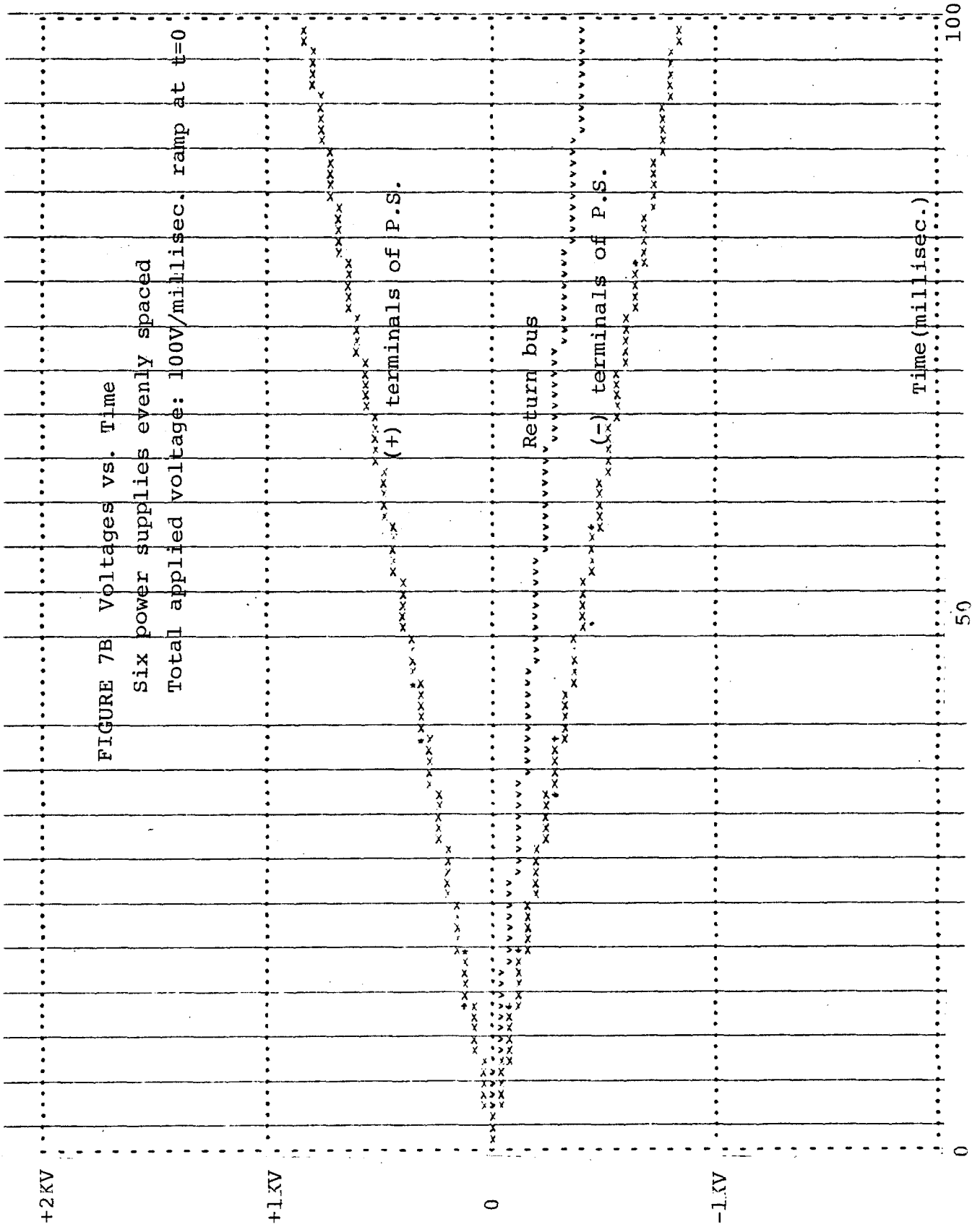


FIGURE 7A Currents vs. Time
Six power supplies evenly spaced
Total applied voltage: 100v/millisec ramp at t=0
160 ohms/cell external damping resistor
Current parabola

Currents (Amps)

Time (millisec.)



50

100

